HYDROLOGICAL PROCESSES
Hydrol. Process. (2010)
Published online in Wiley Online Library
(wileyonlinelibrary.com) DOI: 10.1002/hyp.7885

Modelling plant canopy effects on annual variability of evapotranspiration and heat fluxes for a semi-arid grassland on the southern periphery of the Eurasian cryosphere in Mongolia

Yinsheng Zhang,[1,2]* T. Ohata,[2] J. Zhou[3] and G. Davaa[4]

[1] *Key Lab. of Tibetan Environment Changes and Land Surface Processes, Institute of Tibetan Plateau Research, Chinese Academy of Sciences, Beijing 100085, China*
[2] *Institute of Observational Research for Global Change, Yokosuka 237-0061, Japan*
[3] *Cold and Arid Regions Environmental and Engineering Research Institute, Chinese Academy of Sciences, Lanzhou 730000, China*
[4] *Institute of Meteorology and Hydrology, Ulan Bator, Mongolia*

Abstract:

The ability to predict vegetation cover effects on thermal/water regimes can enhance our understanding of canopy controls on evapotranspiration. The Simultaneous Heat and Water (SHAW) model is a detailed process model of heat and water movement in a snow–residue–soil system. This paper describes provisions added to the SHAW model for vegetation cover and simulation of heat and water transfer through the soil–plant–air continuum. The model was applied to four full years (May 2003–April 2007) of data collected on sparse grassland at Nalaikh in north-eastern Mongolia. Simulated soil temperature and radiation components agreed reasonably well with measured values. The absolute differences between simulated and measured soil temperatures were larger at both the surface layer and deeper layer, but relatively smaller in the layer from 0·8 to 2·4 m. Radiation components were mimicked by the SHAW model with model efficiency (ME) reaching 0·93–0·72. Latent and sensible heat fluxes were simulated well with MEs of 0·93 and 0·87, respectively. The vegetation control on evapotranspiration was investigated by sensitivity experiments of model performance with changing leaf area index (LAI) values but constant of other variables. The results suggest that annual evapotranspiration ranged from 16 to −22% in response to extremes of doubled and zero LAI. Copyright © 2010 John Wiley & Sons, Ltd.

KEY WORDS evapotranspiration; Mongolia; semi-arid grassland; SHAW model

Received 19 February 2010; Accepted 2 September 2010

INTRODUCTION

Vegetation cover can affect the spatial and temporal variabilities of temperature and water in the soil, particularly within a few centimeters of the surface. Knowledge of conditions near the soil–atmosphere interface is of key interest to many areas of research, including studies of seedling germination, plant establishment, insect population dynamics, water conservation, soil freezing, infiltration, runoff and groundwater seepage. The ability to predict heat and water transfer within the soil–plant–atmosphere system enhances our ability to evaluate management options. Models that simulate vegetative cover and plant growth are available (Watts and Hanks, 1978; Tillotson and Wagenet, 1982; Williams *et al*., 1985; Stockle and Campbell, 1989), including some developed for sparse vegetative cover (van Bavel *et al*., 1984; Lascano *et al*., 1987; Horton, 1989). However, most lack detail in modelling water transport through the soil–plant–air continuum or do not include a detailed, mechanistic approach to simultaneous heat and water (SHAW) transfer through snow, residue and soil (frozen and unfrozen), necessary for wintertime simulation.

Researchers have struggled with describing heat and mass transfer between the atmosphere and vegetated surfaces for more than 35 years (Waggoner and Reifsnyder, 1968) and have developed a number of models ranging widely in complexity (Goudriann and Waggoner, 1972; Norman, 1979; Shuttleworth and Wallace, 1985; Kustus, 1990; Massman and Weil, 1999). Comprehensive models capable of simulating microclimate within the canopy typically employ one of two theories. Gradient (or K-theory) models (Norman, 1979; Flerchinger *et al*., 1998; Mihailović *et al*., 2002) define heat and mass fluxes within the canopy as the product of a concentration gradient and the eddy diffusivity, K. Considerable effort has been expended to estimate eddy diffusivities within the canopy (Ham and Heilman, 1991; Jacobs *et al*., 1992; Huntingford *et al*., 1995; Sauer *et al*., 1995; Sauer and Norman, 1995).

However, K-theory has come under criticism for not predicting counter-gradient fluxes (Denmead and Bradley, 1985). Lagrangian trajectory theory (L-theory)

* Correspondence to: Yinsheng Zhang, Key Lab. of Tibetan Environment Changes and Land Surface Processes, Institute of Tibetan Plateau Research, Chinese Academy of Sciences, Beijing 100085, China.
E-mail: yszhang@itpcas.ac.cn

(Raupach, 1989) has been proposed as an alternate to K-theory, and recently several L-theory models have been developed (van den Hurk and McNaughton, 1995; Massman and Weil, 1999; Warland and Thurtell, 2000). Wilson *et al*. (2003) compared K-theory and L-theory approaches and concluded that both approaches performed equally in simulating surface energy components.

The SHAW model, which is based on K-theory, was originally developed by Flerchinger and Saxton (1988) and modified by Flerchinger and Pierson (1991) to include transpiring plants and a plant canopy. The SHAW model differs from most models which simulate the surface energy balance in that transpiration is linked mechanistically to soil water by computing flow through plant roots and leaves within the soil–plant–atmosphere continuum, while satisfying a leaf energy balance. The model has the capability to simulate heat and water transfer through a multispecies canopy and directly computes soil evaporation separately from transpiration. The plant canopy is divided into layers, and evaporation from the soil is computed directly by solving heat and water transfer through each layer within the canopy. Numerous studies have been conducted to test various aspects of the SHAW model, including variability of soil temperature and moisture due to vegetation effects (Flerchinger and Pierson, 1991), snowmelt and soil freezing (Flerchinger and Hanson, 1989; Flerchinger and Saxton, 1989; Flerchinger *et al*., 1994; Hayhoe, 1994) and evaporation.

Grassland covers more than 80% of Mongolian territory. Ma *et al*. (2003) has clarified north-eastern Mongolia to be semi-arid region with higher potential evaporation and lower wetness index. Vegetation cover development in such semi-arid region has been demonstrated variable both in temporal and spatial, and strongly depends on the quantity plus the seasonal and geographical distribution of precipitation (Shinoda *et al*., 2007; Iwasaki, 2009). Miyazaki *et al*. (2004) have documented that the precipitation and soil moisture before July had the most influence on grass growth in central Mongolia, and there is close relation of evapotranspiration and ground surface condition, known as leaf area index (LAI) and soil moisture.

Since July 2002, eco-hydrological observations have been conducted at a sparse grassland site in Mongolia (Zhang *et al*., 2005). The site is locating on the southern periphery of the Eurasian cryosphere region, that the surface heat/water budget is anticipated to be affected by soil shaw–freezing cycle. Variability of evapotranspiration has been elucidated in daily and seasonal scale from the observational studies (Zhang *et al*., 2005, 2007). However, control of vegetation variability on evapotranspiration still poor understood due to the observational researches still too short to elucidate the processes in annual scale. The purpose of this study was to investigate plant canopy effects on annual variability of evapotranspiration by simulating heat and water movement through the soil–plant–air continuum using SHAW model. The model was applied to four full years of data collected on semi-arid grassland with and without vegetation cover. Simulations were compared with measurements from Nalaikh, Mongolia. Sensitivity experiments were also performed to investigate the effects of grass production on evapotranspiration.

MATERIALS AND METHODOLOGY

Model descript

The physical system described by the SHAW model consists of a vertical, one-dimensional profile extending from the vegetation canopy, snow, residue or soil surface to a specified depth within the soil. The system is represented by integrating the detailed physics of a plant canopy, snow, residue and soil complex into one simultaneous solution. Interrelated heat, water and solute fluxes are computed throughout the system, and include the effects of soil freezing and thawing. Net radiation is determined by computing solar and long-wave radiation exchange between canopy layers, residue layers and the soil surface, and considers the direct radiation as well as the upward and downward diffuse radiation transmitted, reflected and absorbed by each layer. Sensible and latent heat fluxes of the surface energy balance are computed from temperature and vapour gradients between the canopy surface and the atmosphere using a bulk aerodynamic approach with stability corrections. Further description of the model may be found in Flerchinger and Saxton (1989) and Flerchinger and Pierson (1991).

Input to the SHAW model includes: initial snow depth and density; initial soil temperature and water content profiles; daily or hourly weather conditions (temperature, wind speed, humidity, precipitation and solar radiation); general site information and parameters describing plant cover, snow, residue and soil. General site information includes slope, aspect, latitude and surface roughness parameters. Plant parameters include LAI, plant height, rooting depth and albedo. Residue or litter properties include residue loading, thickness of the residue layer, percentage cover and albedo. Input soil parameters are bulk density, saturated conductivity, coefficients for the metric potential–water content relation and albedo–water content relation. Outputs from the model include surface energy flux, water balance (including evaporation, transpiration, runoff and deep percolation), soil frost depth, snow depth and soil profiles of temperature, total water content, ice content and solute concentration.

Instruments and measurements

An automatic climate observation system (ACOS) recorded air temperature, humidity and wind speed at heights of 0·5, 1·0, 2·0 and 4·0 m above the ground surface. Shortwave radiation, long-wave radiation and photosynthetically active radiation (PAR) were measured in both upward and downward directions. In addition, sensors measuring air pressure and an infrared radiation thermometer recording grass leaf temperature and

Table I. Instruments used in this study

Item	Unit	Instrument (model, manufacturer)	Record interval
Shortwave radiation	W m^{-2}	Radiometer (MS402, EKO, Japan)	10 min
Long-wave radiation	W m^{-2}	Infrared radiometer (MS202, EKO, Japan)	10 min
All-wave net radiation	W m^{-2}	Net radiometer (Q7, REBS, Inc., USA)	10 min
Photosynthetically active radiation (PAR)	μE s^{-1} m^{-2}	Optical photon-meter (PAR-01, REBS, Inc., USA)	10 min
Wind speed	m s^{-1}	Anemometer (AC750, Kaijo Corporation, Japan)	10 min
Wind direction	deg	Anemometer (VR036, Kaijo Corporation, Japan)	10 min
Snow depth	cm	Ultrasonic level-meter (SR50, CSI, USA)	60 min
Precipitation	mm	Tipping bucket rain gauge (52202, R. M. Young Co., USA)	10 min
Air temperature	°C	Humidity and temperature probe (HMD45D, Vaisala Oyj, Finland) with ventilation pipe (PVC-02, PREDE, Japan)	10 min
Relative humidity	%	Humidity and temperature probe (HMD45D, Vaisala Oyj, Finland) with ventilation pipe (PVC-02, PREDE, Japan)	10 min
Surface temperature	°C	Infrared radiation thermometer (CML303F, CLIM., Inc., Japan)	10 min
Heat flux in the soil	W m^{-2}	Heat flux plate (PHF01, REBS, Inc., USA)	10 min
Volumetric water content	M^3 m^{-3}	ECHO probe (EC-10, Decagon Devices, Inc. USA)	10 min
Soil temperature	°C	Pt-thermometer (TPT100S, CLIMATEC, Inc., Japan)	10 min
Air pressure	hPa	Analog barometer (PTB101B, Vaisala Oyj, Finland)	10 min
Friction wind velocity	m s^{-1}	Ultrasonic Anemometer (CSAT3, CSI), Campell, USA)	10 min
Latent and sensible heat	W m^{-2}	Ultrasonic Anemometer (CSAT3, CSI), Campell, USA)	10 min

net radiation were installed 1·5 m above the ground surface. The eddy covariance method was used to measure latent heat, sensible heat and friction wind speed at 2 m above the ground. We used an open-path hygrometer/H_2O sensor (KH_2O, Campbell, USA) and a three-dimensional supersonic anemometer (81000, Young, USA). Table I provides details of other instruments used in this study. The data presented were collected during the four study years (2003–2007); however, the eddy covariance measurement was conducted during only the grass growth period of 2004.

The eddy covariance system measured the latent and sensible heat fluxes and used three 10 min average flux values to determine one 30 min average. No corrections were performed on data to account for sensor separation, because calculations indicated adjustments to the fluxes of less than 3%. The eddy covariance measurement was conducted just during the grass growth period of 2004. Therefore, result of eddy covariance measurement was just used for verifying simulation results in this work and the parameters estimation in aerodynamics formulas were achieved from as descript by Zhang *et al.* (2007).

Precipitation gauges often underestimate true precipitation amounts. Zhang *et al.* (2004) estimated the downward bias of gauge-measured annual precipitation to be between 17 and 42% in Mongolia. Yokoyama *et al.* (2003) detailed the bias of the gauge used in this study; our precipitation data have been corrected using their procedure, which anticipated a bias of 17%.

Soil moisture was observed both automatically and manually. Seven time-domain reflectometry (TDR) probes and seven Pt thermometers were installed at depths of 0, 0·2, 0·4, 0·8, 1·2, 2·4 and 3·0 m; two sets of heat flux meters were also inserted at 0·02 and 0·2 m. Along with a data logger, these sensors made up the soil monitoring system (SMS). Soil moisture in the surface layer (0–60 cm) was also manually sampled to calibrate the TDR data.

Phenological observations, including those of the grass coverage and biomass and the water content of grass leaves, were conducted at 10-day intervals during the study period at four 50 × 50 cm plots. The results have been analysed in previous publications (Zhang *et al.*, 2005, 2007).

Model simulation

The model was run without prior calibration at study site for a period of four complete years from May 2003 to April 2007. Using observed data as forcing input, heat and water transfer were simulated for a 2 m profile above ground surface and 3 m in the ground. Hourly weather conditions above the upper boundary and soil conditions at the lower boundary define heat and water fluxes into the system. A layered system is established through the vegetation canopy, snow, residue and soil, with each layer represented by a node. After computing flux at the upper boundary, the interrelated heat, liquid water and vapour fluxes between layers are determined. Heat and water flux for the system are computed simultaneously using implicit finite difference equations and solved iteratively using a Newton–Raphson procedure. In this work, soil temperature for the lower boundary of the 300 cm profile was assumed constant and equal to the average air temperature (0·3 °C) for the simulation period. A constant water potential of −2·0 m was assumed at the 300 cm depth based on observed soil properties.

Measured plant height, LAI and rooting depth were used to parameterize the model, detail parameterization can referee to Flerchinger and Pierson (1991). Parameters for total root resistance r_r, total leaf resistance r_l (stomatal plus leaf boundary layer resistance) and unstressed stomatal resistance r_{so} for the grass were estimated to be $1{\cdot}7 \times 10^6$ m^3 s kg^{-1}, $6{\cdot}7 \times 10^5$ m^3 s kg^{-1}

and 100 s m^{-1}, respectively, following to Flerchinger *et al*. (1996). Critical leaf potential Ψ_c and the stomatal resistance exponent were given as −100 m and 5 (Flerchinger and Pierson, 1991), respectively, and the albedo of the grass was set to 0·18 (as described in '*Site Description*' section).

Simulated and measured values were compared using several coefficients of efficiency (Xiao *et al*., 2006):

$$\mathrm{ME} = 1 - \frac{\sum[Y(i) - Ys(i)]^2}{\sum[Y(i) - \overline{Y}(i)]^2} \quad (1)$$

$$\mathrm{RMSD} = \left\{ \frac{1}{N} \sum_{i=1}^{N} [Ys(i) - Y(i)]^2 \right\}^{1/2} \quad (2)$$

$$\mathrm{MBE} = \frac{1}{N} \sum_{i=1}^{N} [Ys(i) - Y(i)] \quad (3)$$

where $Y(i)$ is a measured value, $Ys(i)$ is a corresponding simulated value and $\overline{Y}(i)$ is the average measured value for the simulation period. RMSD is the root mean-square deviation between simulated and observed values, MBE is the mean bias error of SHAW model predictions compared to observed values and ME is the model efficiency, that is, the variation in measured values accounted for by the model, which implies the fraction of variation in measured values explained by the model. ME is similar to the coefficient of determination used for regression models, except that ME can be negative. Negative values of ME indicate that the average measured value for the period is a better estimate of measured values than are simulated values.

Site description

The experiment was conducted on sparse grassland at Nalaikh in north-eastern Mongolia (47°45′N, 107°20′E), 40 km southeast of Ulaanbaatar. The site was located on a sediment plain in the broad Tuul River valley (Figure 1). The nearest mountains, with relative heights of less than 500 m, were at least 10 km away, and the topography at and around this site was very smooth.

The surface soil in the study region is sandy, contains little organic matter, and is less than 10 cm thick. Large sand grains occur beneath the surface layer with a bulk density of 1·1–1·7 g cm^{-3} and porosity of 32–59% (Zhang *et al*., 2005).

The observation site was in a semi-arid region characterized by warm, dry summers (Bereneva, 1992). Figure 2 presents observed daily air temperature, precipitation, net radiation and albedo for May 2003 to April 2007. The annual air temperature and that averaged for the plant growth season (May–September) were −4·2 °C and 2·3 °C, respectively. Annual precipitation averaged 224 mm with a range of 190–250 mm, and 75–90% of precipitation occurred in the growth season, implying a dry condition and heterogeneous temporal distribution of precipitation.

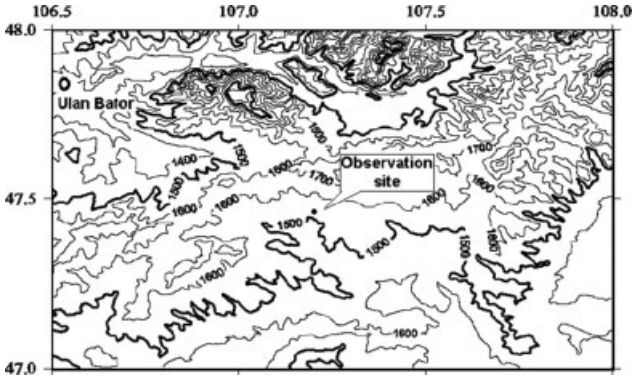

Figure 1. Map of the observation site

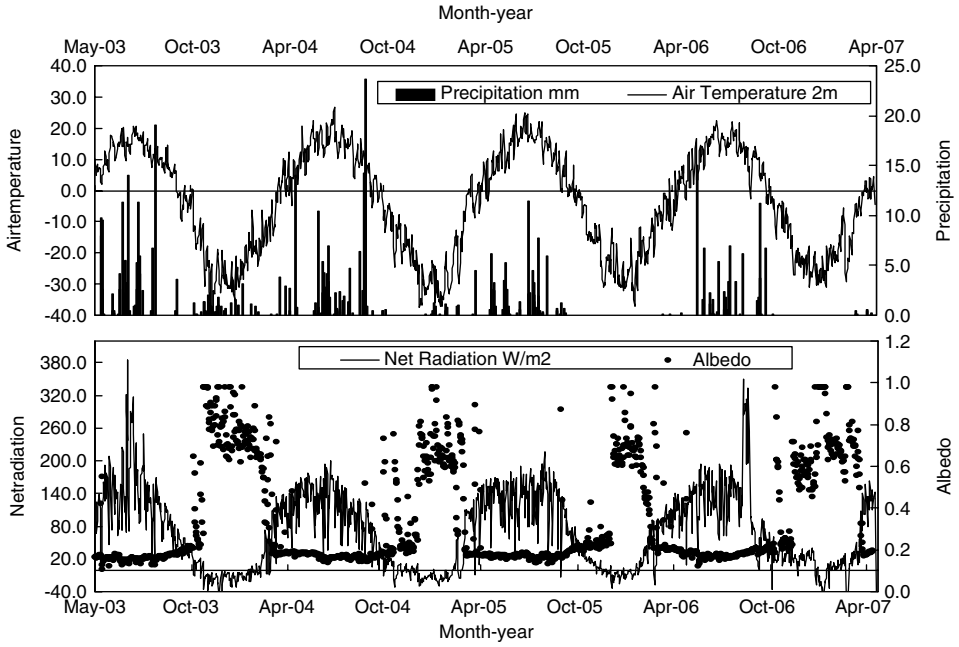

Figure 2. Variations of daily air temperature, precipitation, net radiation and albedo at the study site from May 2003 to April 2007

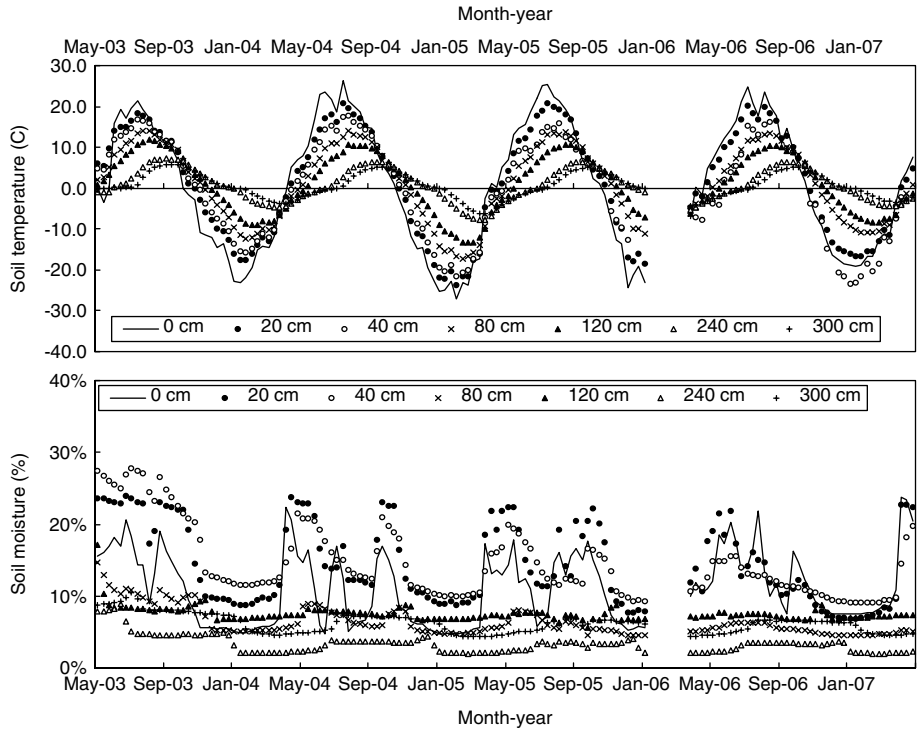

Figure 3. Variation of daily soil temperature and moisture at 0·0, 0·2, 0·4, 0·8, 1·2, 2·4 and 3·0 m depth in the period from May 2003 to April 2007 at the study site

Net radiation averaged 64·7 W m^{-2} and was temporally negative in mid-winter, in accordance with peak albedo of nearly 1·0 (Fig. 2). The albedo averaged 0·20 in the snow-free period with a minimum of 0·18, which was treated as dry soil albedo in the simulation.

Ishikawa *et al*. (2005) has classified the permafrost at study as 'warm permafrost'. The soil temperature plotted in Figure 3 reveals a thick active layer and higher ground surface temperatures characterize permafrost regions at the study site. Observations of ground temperature from the surface to a depth of 3 m showed that the surface temperature was continuously below 0 °C at the beginning of October. The downward frost front moved from the surface to 3 m in the following 85–90 days. After the snow cover disappeared at the beginning of April, the surface started to melt. The downward-moving thawing front reached 3 m in the mid-May. Seasonal variation of the permafrost active layer suggests that the thaw–frost cycle may not affect biological processes of the grass because the thaw depth exceeded 3 m during the growth period (May–September), although the study site was underlain by permafrost. The soil water content deeper than 120 cm was generally low throughout the summer, varying less than 7%; furthermore, soils during the following winter period had low ice content. The winter soils might have been warmed by thickened snow cover that reduced the heat exchange with the atmosphere (Ishikawa *et al*., 2005).

Vegetation was uniformly sparse grass with coverage of 38–60% during the maximum growth period. Over pasture, plant types and species did not vary. *Artemisia frigida* dominated (∼60%), and other species included *Arenaria* and *Leymus chinensis*. The maximum grass height in mid-July was less than 20 cm. Root investigation showed the grass roots develop mainly in the surface ground layer (the top 50 cm). Differences in root biomass between April and June also occurred only in the ground surface layer, which suggests that the root zone at the study site was the layer between the soil surface and 50 cm depth (Zhang *et al*., 2005).

SIMULATION RESULTS

Table II summarizes the model performance measures for soil temperature at all observed depths, whereas Figure 4 gives examples of regression analysis results for depths of 0·0, 0·2, 0·4 and 0·8 m. The ME for the depths less than 1·2 m ranged from 0·91 to 0·96, indicating that the model captured most of the variation in measured values; however ME dropped to 0·65 and −0·31 for depths of 2·4 and 3·0 m, respectively. The drop in efficiency at the deeper depth was undoubtedly caused by the assumption of a constant temperature at the bottom of simulating layer at depth of 3 m in this work. Such an assumption is necessary in modelling work when dealing with the soil freeze/thaw cycle, even if

Table II. Model performance measures for soil temperature (°C)

Depth	0·0 m	0·2 m	0·4 m	0·8 m	1·2 m	2·4 m	3·0 m	Mean
ME	0·93	0·96	0·92	0·93	0·91	0·65	−0·31	0·71
RMSD	1·63	1·10	1·34	0·94	0·88	0·95	1·43	1·18
MBE	−0·65	−0·84	0·21	−0·77	−0·75	−0·79	−0·90	−0·64

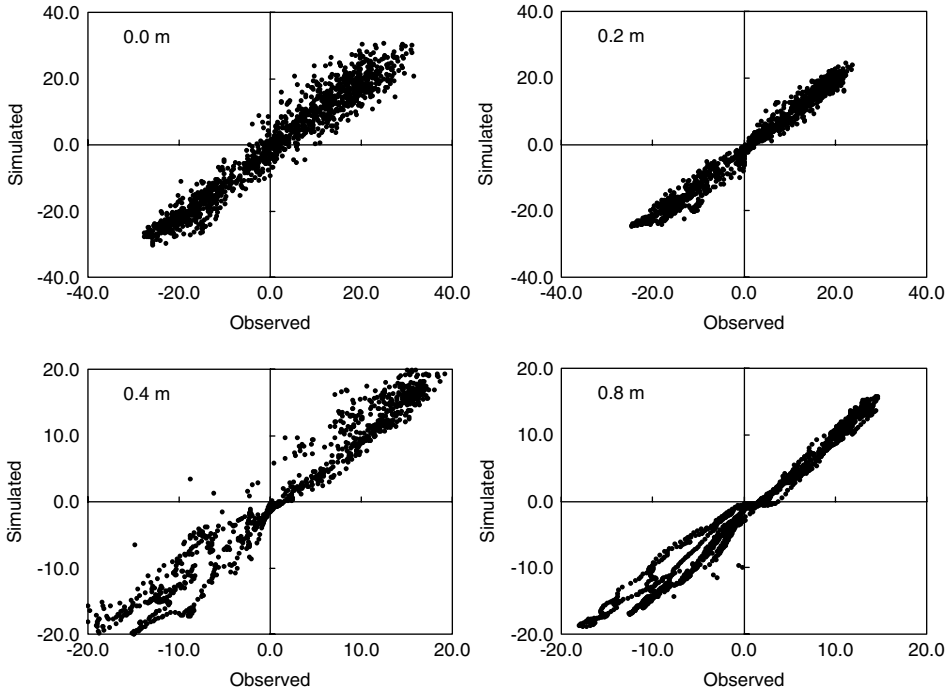

Figure 4. Simulated *versus* measured average daily soil temperature (°C) at depths of 0·0, 0·2, 0·4 and 0·8 m

some annual variation would have existed realistically (Ishikawa *et al*., 2005).

The RMSD shows that the absolute difference between simulated and measured soil temperatures was larger at both the surface layer and deeper layer, but relatively smaller in the depth range from 0·8 to 2·4 m. The MBE reveals that soil temperature was also systematically underestimated at 0·4 m depth. The cause of this underestimation during the study period is not known and could have arisen from a variety of factors. Possible reasons include a change in soil albedo during this period due to a change in water content or the sun's declination angle; inaccurate calculation of soil thermal conductivity for the very dry soil during this period; and inaccurate estimation of surface roughness parameters causing an overestimation of sensible heat transfer, which is estimated from observed plant canopy height (Flerchinger and Pierson, 1991).

The soil moisture was measured at multiple depths as same as soil temperature, simulating results were statistically evaluated at all measuring depth in Table III, but compared in Figure 5 just at surface and 3 m. The ME for simulated soil moisture was 0·99 and 0·83 at 1·2 and 3·0 m. RMSDs for the four years were slightly greater than 6% beside at the surface. The negative MBE reveals that soil moisture was systematically underestimated at most depths. The largest differences between the measured and modelled values of soil moisture occurred during the winter months (Figure 5), the measured soil moisture was systematically lower than that of modelled. Some previous work elucidated such kind of overestimate on soil moisture during winter is because of errors in the simulation of the timing and rate of snow-cover deposition and ablation (Link *et al*., 2004). However, errors of the TDR probe measuring soil moisture during frozen is anticipated main cause of error shown in Figure 5. As Zhang *et al*. (2004) demonstrated that what TDR recorded is soil liquid water content, but SHAW model output soil moisture in totally (Flerchinger and Saxton, 1989).

Table III. Model performance measures for soil moisture (m^3/m^3)

Depth	0·0 m	0·2 m	0·4 m	0·8 m	1·2 m	2·4 m	3·0 m	Mean
ME	0·21	−0·05	−0·03	0·56	0·99	−0·87	0·83	0·23
RMSD	0·13	0·05	0·02	0·04	0·02	0·06	0·01	0·05
MBE	0·00	−0·03	−0·03	−0·03	−0·02	−0·05	0·00	−0·02

Time series of simulated and measured components of radiation balance, including shortwave, long-wave and all-wave net radiation, from May 2003 to April 2007 are plotted in Figure 6. The ME values for shortwave, long-wave and all-wave net radiation were 0·93, 0·75 and 0·72, respectively. Shortwave radiation clearly was simulated more reasonably than was long-wave radiation. MBE for long-wave radiation was 3·1 W m^{-2} with RMSD of 15·2 W m^{-2}, which is significantly larger than that of shortwave radiation, which had MBE of −1·5 W m^{-2} and RMSD of 10·2 W m^{-2}. The worst simulation result was for all-wave net radiation, which would logically include the contribution of the simulated long-wave radiation. Some studies have reported overestimation of long-wave radiation by the SHAW model, but the cause has not been well understood (*Denmead and Bradley*, 1985). In the SHAW model, long-wave emittance by a canopy layer is calculated using a leaf temperature for all plant species that is equal to the air temperature within the layer; thus emitted long-wave radiation is

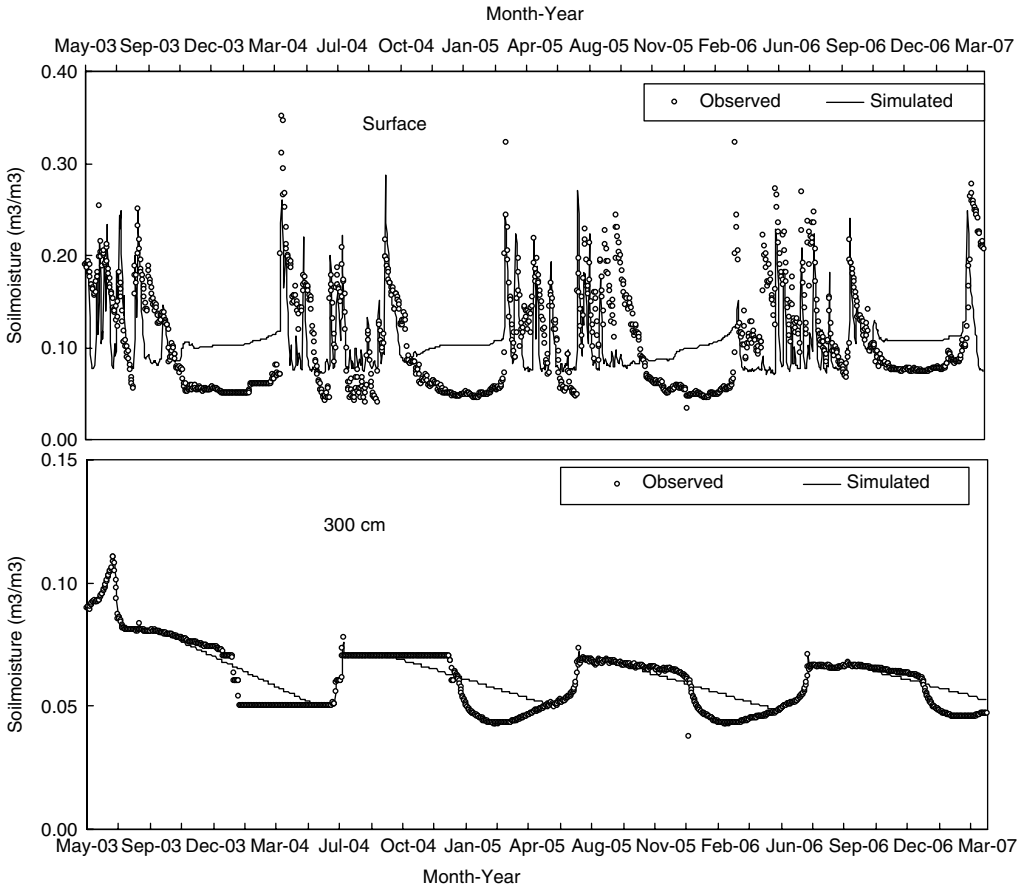

Figure 5. Simulated *versus* measured average daily soil moisture (m^3/m^3) at depths of 0·0 and 3·0 m

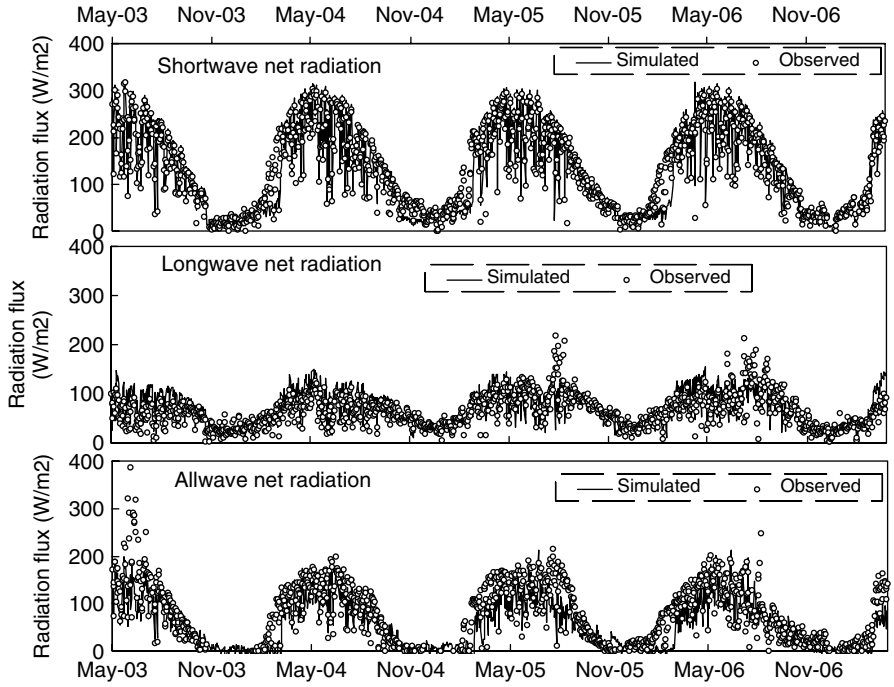

Figure 6. Measured and simulated daily shortwave, long-wave and all-wave net radiation for grassland in Nalaikh from May 2003 to April 2007

biased by the difference between air temperature and leaf temperature.

The simulations of sensible and heat flux were evaluated based on the eddy covariance measurements conducted during the grass growth period of 2004 (20 May–29 August). Figure 7 plots simulated *versus* measured daily latent heat and sensible heat fluxes during the period. The simulated latent heat and sensible heat fluxes

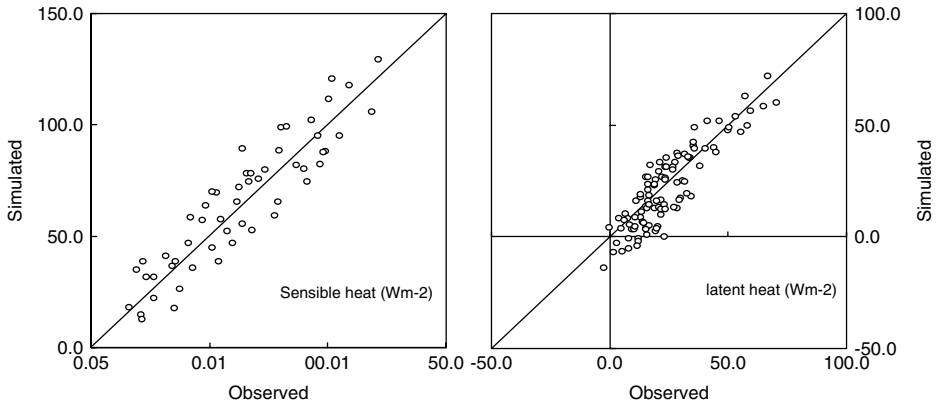

Figure 7. Simulated *versus* measured daily latent heat and sensible heat flux from 20 May to 29 August 2004

Table IV. Average measured values, model efficiency (ME), root mean-square deviation (RMSD), and mean bias error (MBE) for components of the surface energy balance averaged for clear and rainy days during 20 May–29 August, 2004

	Average (W m^{-2})	ME	RMSD	MBE (W m^{-2})
	Clear-day			
Shortwave net radiation	211·3	0·99	11·4	6·8
Long-wave net radiation	90·4	0·63	23·9	12·1
All-wave net radiation	110·9	0·60	12·0	−4·8
Sensible heat	63·0	0·93	12·0	2·5
latent heat	19·8	0·82	9·2	−3·1
	Raining-day			
Shortwave net radiation	165·2	0·92	16·4	3·5
Long-wave net radiation	62·7	0·50	16·5	7·2
All-wave net radiation	102·5	0·54	15·4	−4·1
Sensible heat	64·4	0·94	11·5	−3·4
Latent heat	33·3	0·96	7·3	−0·6

agreed well, with ME values of 0·93 and 0·87, respectively. However, latent heat flux was underestimated with MBE of −2·3 W m^{-2} and RMSD of 8·46 W m^{-2}, and sensible heat flux was overestimated with MBE of 1·8 W m^{-2} and RMED of 11·88 W m^{-2}.

To examine whether precipitation influenced model performance, Table IV presents ME, RMSD, MBE and observed values averaged for clear days and rainy days. Model performance for radiation components, including shortwave, long-wave and all-wave net radiation, changed little. The ME increased from 0·82 to 0·96 for latent heat flux, but fewer changes were found for sensible heat flux. Both all-wave net radiation and latent heat flux were underestimated regardless of whether rainy days were included. Sensible heat flux was underestimated for rainy days, but overestimated for clear days, as shown by the MBE in Table IV. The difference in MBE values suggests that precipitation events affect the accuracy of the measurement, the model simulation or both.

DISCUSSION

Evapotranspiration over an ecosystem consists of soil evaporation (E_{soil}) and vegetation transpiration (E_{trans}), and controls on the variability of these two processes are different. In this work, to examine vegetation control on evapotranspiration variability, we conducted a sensitivity experiment of modelling performance; the experiment involved changing the grass LAI by +100, +50, −50, −75 and −100% (representing evaporation from bare soil) without changing any other variables in the model. E_{trans}, then, could be estimated from the difference between total evapotranspiration and E_{soil}.

Interannual changes of evapotranspiration and ground water condition

Zhang *et al.* (2005, 2007) investigated environmental controls on evapotranspiration from sparse grassland on daily and seasonal time scales by separating E_{soil} and E_{trans} from total evapotranspiration. At the present study site, the seasonality of evapotranspiration has been shown to be dominated by radiation forcing, which is generally associated with potential evapotranspiration (E_p), which calculated by Penman method as described by (Zhang *et al.*, 2007). Normalized soil evaporation (E_{soil}/E_p) is a good measure for evaluating the response of evapotranspiration to the surface water condition, especially in a semi-arid environment; evidence is provided by the temporal decline of evapotranspiration from grasses and the ratio of E_{soil}/E_p, which relates to precipitation events or snow melting. At time scales shorter than a season, only a slight anticipated effect of vegetation on evapotranspiration was suggested and thus an exact effect could not be deduced.

To examine the annual variability in evapotranspiration as associated with the ground surface water condition, variation of mean E_{soil}/E_p *versus* precipitation and the integrated E_{trans} *versus* soil moisture at 40 cm depth for growth seasons (May–October) of 2003–2006 at the study site are plotted in Figure 8. The temporal pattern of E_{soil}/E_p, denoting the response of evapotranspiration to the water condition, differs at annual and seasonal time scales (Zhang *et al.*, 2005). E_{soil}/E_p shows large increase when summer precipitation exceeds 150 mm, but generally little variation for summer precipitation less than 150 mm. At the seasonal scale, E_{soil}/E_p has been found to be rather sensitive to soil moisture in the range of

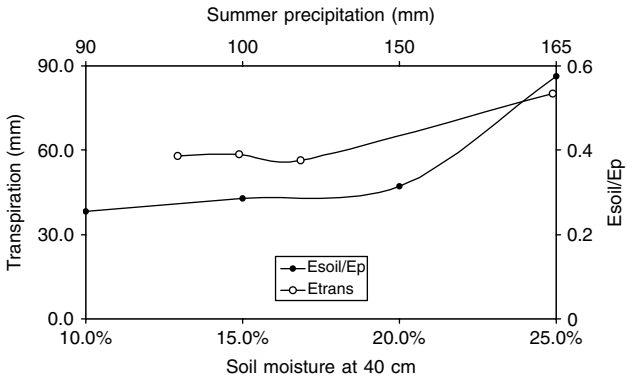

Figure 8. Variation of mean E_{soil}/E_p *versus* precipitation and the sum of E_{trans} *versus* soil moisture at 40 cm depth for the growth seasons (May–October) of 2003–2006

10–20%, but Figure 8 reveals few changes of E_{soil}/E_p in the soil moisture range of 10–20%. E_{trans}, which has been demonstrated to be affected by deeper soil moisture but not by that at the surface on a seasonal scale (Zhang *et al*., 2007), shows a significant increase when soil moisture at 40 cm depth is larger than 20%, but only slight variation when soil moisture is lower than 20%. Note that soil moisture of 20% is a critical value in soil hydrology as it is roughly equivalent to the field water capacity (Zhang *et al*., 2007).

Canopy control on evapotranspiration

To understand canopy control on the annual variability of evapotranspiration at the study site, Figure 9 plots the variation of soil evaporation (E_{soil}), transpiration (E_{trans}), total evapotranspiration (E_{total}) and soil moisture at 20 cm *versus* the ratio of grass LAI changing from 2003 to 2006. E_{soil} increased 20% when LAI doubled (100%), but decreased 25% as LAI changed by −75% and showed no change as LAI decreased from −75 to −100% (bare soil). E_{total} increased 16% as LAI doubled, decreased to its minimum value as LAI decreased by 25%, and increased very slightly by 1% as LAI changed from −75% to bare soil (−100%). E_{trans}, the key component denoting canopy control on evapotranspiration, increased 80% when LAI doubled and decreased 92% when LAI was cut in half. E_{trans} become zero with an LAI decrease of 75%, implying that 25% present LAI might be the level at which vegetation has an effect on evapotranspiration at the study site. E_{trans} had an extreme annual value of 80 mm and made up less than 30% of total evapotranspiration, as also shown by observations at the study site (Zhang *et al*., 2005). Changes ranging from +17 to −22%, in accordance with doubled LAI and bare soil, respectively, are expected to be the extremes of canopy effects in the annual evapotranspiration range. The cause of this change is rather complex as demonstrated by Zhang *et al*. (2005, 2007). In such semi-arid region, soil moisture is main factor to control total evapotranspiration as shown in Figure 9. However, E_{total} has been addressed to be varied with various factors including surface energy budget, what soil moisture dominated is E_{soil}, but not E_{trans} (Zhang *et al*., 2007).

The sum of the net solar and net long-wave radiation to the changing LAI plotted in Figure 10 gives the all-wave net radiation balance for the site, also plotted in Figure 10. Latent heat fluxes varied with LAI, which tend to dominated by net all-wave net radiation. Net shortwave radiation was small much of the time and had less variation with changing LAI than any other component of the radiation balance. In contrast, long-wave radiation budget is strongly dependent on LAI, which ranged −5 to 10% in accordance to LAI changed 100 to −100%. Thus, the variation of latent heat (indicating variation of E_{total}) is anticipated elucidated by changing in long-wave radiation budget with LAI. Emitted long-wave radiation theoretical is strongly dependent on surface temperature, it is not surprising that long-wave radiation budget was also strongly dependent on LAI. Genxu *et al*. (2009) have demonstrated that surface temperature was efficiently affect by vegetation condition by observational results on Tibetan Plateau.

SUMMARY

The SHAW model is a process model of heat and water transfer in a snow–residue–soil system which integrates

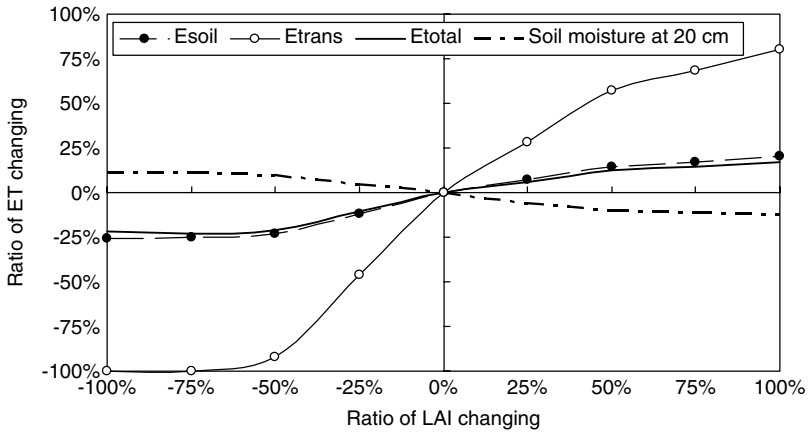

Figure 9. Variation of soil evaporation (E_{soil}), transpiration (E_{trans}), total evapotranspiration (E_{total}) and soil moisture at 20 cm *versus* the ratio of grass LAI changing during 2003–2006

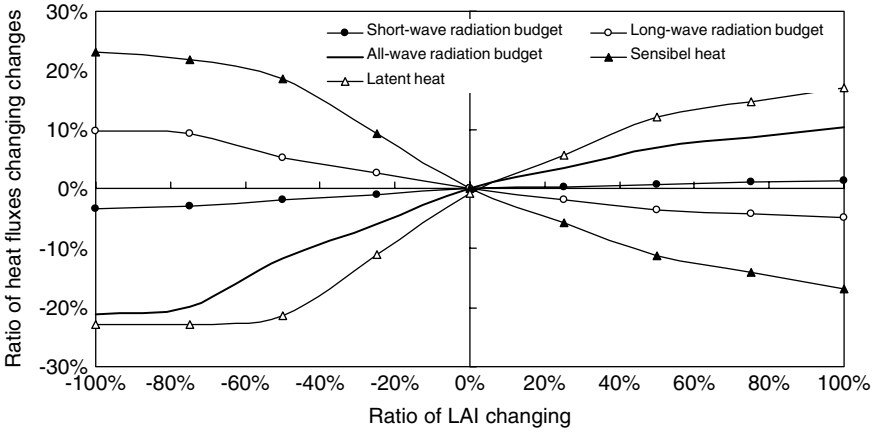

Figure 10. Variation of shortwave radiation budget, long-wave radiation budget, all-wave radiation budget and latent and sensible fluxes versus the ratio of grass LAI change during 2003–2006

the detailed physics of snow, residue and soil (frozen and unfrozen) into one simultaneous solution. Additions were made to the model to accommodate the effects of plant cover on heat and water movement. The framework of the detailed mathematical model of heat and water transfer through a plant canopy is presented in this work. The SHAW model was applied to four full years of data collected on sparse grassland at Nalaikh in north-eastern Mongolia.

The model was applied without calibration to a 3 m profile, and the resulting simulated soil temperature and radiation components agreed reasonably well with measured values. The absolute differences between simulated and measured soil temperatures were larger at both the surface layer and deeper layer, but relatively smaller at depths from 0·8 to 2·4 m. The bias errors reveal that soil temperatures were also systematically underestimated at 0·4 m depth. The cause of this underestimation for the study period is not understood. More detailed observations and investigations are required.

Radiation components, including shortwave, long-wave and all-wave net radiation, were simulated by the SHAW model with ME values of 0·93–0·72 and MBE less than 10 W m^{-2} for the entire simulation from May 2003 to April 2007. Latent and sensible heat fluxes were simulated well with ME of 0·93 and 0·87, respectively. However, latent heat flux was underestimated with MBE of $-2{\cdot}3$ W m^{-2} and RMED of 8·46, and sensible heat flux was overestimated with MBE of 1·8 W m^{-2} and RMED of 11·8.

Main target of this work is to examine the effects of plant cover on heat and water fluxes in annual time-scale at such semi-arid ground surface with sparse grass cover. Simulating result suggests that temporal pattern of evapotranspiration at an annual scale was different from that at the seasonal scale described by previous works. Improvements could be made in understanding the canopy control on evapotranspiration by sensitivity experiments of model performance with changing LAI. The sensitivity experiments reveal that annual evapotranspiration values ranged from 16 to -22% in response to LAI extremes of doubled and zero LAI; this range shows the amount of canopy coverage that could alter evapotranspiration efficiently through change grass transpiration and also soil evaporation. Surface energy budget is a main factor effect the changing in evapotranspiration with LAI through long-wave radiation exchange processes with variation in surface condition. Simulated water balance implied by beneath soil moisture was decreased, associated with increase of evapotranspiration, with increasing LAI with the range of 11 to -13%. The result may imply negative feedback between soil moisture and vegetation on such semi-arid grass land: increasing in canopy production under climate warming may rising soil water losing due to evapotranspiration process; however, decreasing in soil moisture restrain evaporation processes subsequently.

ACKNOWLEDGEMENTS

Grateful thanks are extended to D. Azzaya, and D. Uyunbaatar for their help and cooperation with our fieldwork in Mongolia.

REFERENCES

Bereneva IA. 1992. In *Ecology and nature management in Mongolia*, Dorofeyuk NI (ed). GUGK MPR: Ulaanbaatar; 25–32. (in Russian).

Denmead OT, Bradley EF. 1985. In *The Forest—Atmosphere Interaction*, Hutchison BA, Hicks BB (eds). Reidel Publ. Co.: Hingham, MA; 412–442.

Flerchinger GN, Hanson CL. 1989. Modeling soil freezing and thawing on a rangeland watershed. *Transactions of American Society of Agricultural Engineers* **32**: 1551–1554.

Flerchinger GN, Pierson FB. 1991. Modeling plant canopy effects on variability of soil temperature and water. *Agricultural and Forest Meteorology* **56**: 227–246.

Flerchinger GN Saxton KE. 1988. *Modeling Agricultural, Forest, and Rangeland Hydrology, Proc. 1988 Int. Syrup*. ASAE Publ. 07–88, *American Society of Agricultural Engineers*: St. Joseph, MI; 176–185.

Flerchinger GN, Saxton KE. 1989. Simultaneous heat and water model of a freezing snow-residue-soil system. I. Theory and development. *Transactions of American Society of Agricultural Engineers* **32**: 565–571.

Flerchinger GN, Cooley KR, Deng Y. 1994. Impacts of spatially and temporally varying snowmelt on subsurface flow in a mountainous watershed: I. Snowmelt simulation. *Hydrological Sciences Journal* **39**: 507–520.

Flerchinger GN, Hanson CL, Wight JR. 1996. Modeling of evapotranspiration and surface energy budgets across a watershed. *Water Resources Research* **32**: 2539–2548.

Flerchinger GN, Kustas WP, Weltz MA. 1998. Simulating surface energy fluxes and radiometric surface temperatures for two arid vegetation communities using the SHAW model. *Journal of Applied Meteorology* **37**: 449–460.

Goudriann J, Waggoner PE. 1972. Simulating both aerial microclimate and soil temperature from observations above the foliar canopy. *Netherlands Journal of Agricultural Science* **20**: 104–124.

Ham JM, Heilman JL. 1991. Aerodynamic and surface resistances affecting energy transport in a sparse crop. *Agricultural and Forest Meteorology* **53**: 267–284.

Hayhoe HN. 1994. Field testing of simulated soil freezing and thawing by the SHAW model. *Canadian Agricultural Engineering* **36**: 279–285.

Horton R. 1989. Canopy shading effects on soil heat and water flow. *Soil Science Society of America Journal* **53**: 669–679.

Huntingford C, Allen SJ, Harding RJ. 1995. An intercomparison of single and dual-source vegetation—atmosphere transfer models applied to transpiration from Sahelian savannah. *Boundary-Layer Meteorology* **74**: 397–418.

Ishikawa M, Sharkhuu N, Zhang Y, Kadota T, Ohata T. 2005. Ground thermal and moisture conditions at the southern boundary of discontinuous permafrost, Mongolia. *Permafrost and Periglacial Processes* **16**: 209–216.

Iwasaki H. 2009. NDVI prediction over Mongolian grassland using GSMaP precipitation data and JRA-25/JCDAS temperature data. *Journal of Arid Environments* **73**: 557–562.

Jacobs AFG, van Boxel JH, Shaw RH. 1992. The dependence of canopy layer turbulence on within-canopy thermal stratification. *Agricultural and Forest Meteorology* **58**: 247–256.

Kustus WP. 1990. Estimates of evaporation with a one- and two-layer model of heat transfer over partial canopy cover. *Journal of Applied Meteorology* **29**: 704–715.

Lascano RJ, van Bavel CHM, Hatfield JL, Upchurch DR. 1987. Energy and water balance of a sparse crop: simulated and measured soil and crop evaporation. *Soil Science Society of America Journal* **51**: 1113–1121.

Link T, Unsworth M, Marks D. 2004. Simulation of water and energy fluxes in an old-growth seasonal temperate rain forest using the simultaneous heat and water (SHAW) model. *Journal of Hydrometeorolgy* **5**: 443–457.

Ma X, Yasunari T, Ohata T, Natsagdorj L, Davaa G, Oyunbaatar D. 2003. Hydrological regime analysis of the Selenge River Basin, Mongolia. *Hydrological Processes* **17**: 2929–2945.

Massman WJ, Weil JC. 1999. An analytical one-dimensional second-order closure model of turbulence statistics and the Lagrangian time scale within and above plant canopies of arbitrary structure. *Boundary-Layer Meteorology* **91**: 81–107.

Mihailović DT, Lalić B, Arsenić I, Eitzinger J, Dusanic N. 2002. Simulation of air temperature inside the canopy by the LAPS surface scheme. *Ecological Modelling* **147**: 199–207.

Miyazaki S, Yasunari T, Miyamoto T, Kaihotsu I, Davaa G, Oyunbaatar D, Natsagdorj L, Oki T. 2004. Agrometeorological conditions of grassland vegetation in central Mongolia and their impact for leaf area growth. *Journal of Geophysics Research* **109**: D22106, DOI:10.1029/2004JD005179.

Norman JM. 1979. Modeling the complete crop canopy. In *Modification of the Aerial Environment of Plants*, *ASAE Monograph,* Barfield BJ, Gerber JF (eds). St. Joseph, MI; 249–277.

Raupach MR. 1989. A practical Lagrangian method for relating scalar concentrations to source distributions in vegetation canopies. *Quarterly Journal of the Royal Meteorological Society* **115**: 609–632.

Sauer TJ, Norman JM. 1995. Simulated canopy microclimate using estimated below-canopy soil surface transfer coefficients. *Agricultural and Forest Meteorology* **75**: 135–160.

Sauer TJ, Norman JM, Tanner CB, Wilson TB. 1995. Measurement of heat and vapor transfer coefficients at the soil surface beneath a maize canopy using source plates. *Agricultural and Forest Meteorology* **75**: 161–189.

Shinoda M, Ito S, Nachinshonhor GU, Erdenetsetseg D. 2007. Phenology of Mongolian grasslands and moisture conditions. *Journal of the Meteorological Society of Japan* **85**: 359–367.

Shuttleworth WJ, Wallace JS. 1985. Evaporation from sparse crops—An energy combination theory. *Quarterly Journal of the Royal Meteorological Society* **111**: 839–855.

Stockle CO, Campbell GS. 1989. Simulation of crop response to water and nitrogen: an example using spring wheat. *Transactions of American Society of Agricultural Engineers* **32**: 66–74.

Tillotson WR, Wagenet RJ. 1982. Simulation of fertilizer nitrogen under cropped situations. *Soil Science* **133**: 133–143.

van Bavel CHM, Lascano RJ, Stroosnijder L. 1984. Test and analysis of a model of water use by sorghum. *Soil Science* **137**: 443–456.

van den Hurk BJJM, McNaughton KG. 1995. Implementation of near-field dispersion in a simple two-layer surface resistance model. *Journal of Hydrology* **166**: 293–311.

Waggoner PE, Reifsnyder WE. 1968. Simulating of the temperature, humidity and evaporation profiles in a leaf canopy. *Journal of Applied Meteorology* **7**: 400–409.

Warland JS, Thurtell GW. 2000. A Lagrangian solution to the relationship between a distributed source and concentration profile. *Boundary-Layer Meteorology* **96**: 453–471.

Watts DG, Hanks RJ. 1978. A soil-water-nitrogen model for irrigated corn on sandy soils. *Soil Science Society of America Journal* **42**: 492–499.

Williams JR, Nicks AD, Arnold JG. 1985. Simulator for water resources in rural basins. *Journal of Hydrologic Engineering, American Society of Civil Engineers* **111**: 970–986.

Wilson TB, Norman JM, Bland WL, Kucharik CJ. 2003. Evaluation of the importance of Lagrangian canopy turbulence formulations in a soil–plant–atmosphere model. *Agricultural and Forest Meteorology* **115**: 51–69.

Xiao W, Qiang Y, Flerchinger GN, Zheng YF. 2006. Evaluation of SHAW model in simulating energy balance, leaf temperature and micrometeorological variables within a maize canopy. *Agronomy Journal* **98**: 722–729.

Yokoyama K, Ohno H, Kominami Y, Inoue S, Kawakata T. 2003. Performance of Japanese precipitation gauges in winter. *Seppyo* **65**: 303–316.

Zhang Y, Munkhtsetseg E, Kadota T, Ohata T. 2005. An observational study of ecohydrology of a sparse grassland at the edge of the Eurasian cryosphere in Mongolia. *Journal of Geophysical Research* **110**: D14103, DOI:10.1029/2004JD005474.

Zhang Y, Ohata T, Yang D, Davaa G. 2004. Bias correction of daily precipitation measurements for Mongolia. *Hydrological Processes* **18**: 2991–3005.

Zhang Y, Kadota T, Ohata T, Oyunbaatar D. 2007. Environmental controls on evapotranspiration from sparse grassland in Mongolia. *Hydrological Processes* **110**: 12016–12027.

